Study of the temperature dependence of isothermal spherulitic growth rate data for poly(pivalolactone) in blends with poly(vinylidene fluoride): a link between coherent secondary nucleation theory and mixing thermodynamics*

Jiang Huang, Abaneshwar Prasad and Hervé Marand†
Department of Chemistry and NSF Science & Technology Center for High Performance Polymeric Adhesives and Composites, Virginia Polytechnic Institute & State University, Blacksburg, VA 24061-0212, USA
(Received 28 July 1993)

The spherulitic growth rates of α-phase poly(pivalolactone) (PPVL) in blends with poly(vinylidene fluoride) (PVF_2) were measured by polarized optical microscopy as a function of blend composition and isothermal crystallization temperature T_x between 160 and 215°C. The PPVL weight fraction in the blends ranges from 100 to 10 wt%, which constitutes the largest compositional range investigated in any such study. Using the Lauritzen–Hoffman kinetic theory of crystallization, the composition dependent equilibrium melting temperatures T_m, the nucleation constants $K_{g(II)}$ and $K_{g(III)}$ and the surface free energy product $\sigma\sigma_e$ were determined directly from the temperature dependence of the spherulitic growth rate data for each blend. The equilibrium melting temperature, the nucleation constants and the product of the fold and lateral surface free energies of PPVL α-phase crystals are observed to decrease with increasing PVF_2 content. The observed depression in equilibrium melting temperature was successfully analysed following the treatment proposed by Nishi and Wang and based on Scott's expression for chemical potentials in a binary polymer mixture to yield a negative interaction parameter ($\chi = -0.13 \pm 0.05$). The magnitude of this interaction parameter is consistent with that found in earlier studies of poly(vinylidene fluoride)/poly(methyl methacrylate) blends. Finally, the observed decrease in crystal/melt surface free energy product is discussed in the context of a recent model correlating the lateral crystal/melt interfacial free energy with the characteristic ratio of the crystallizable polymer chain. Our analysis suggests that the lateral crystal/melt interface thickness should increase with PVF_2 concentration in the blend in order to minimize the demixing of a crystallizable chain as it diffuses into the melt/crystal interface to become physically adsorbed onto the crystal growth front.

(Keywords: poly(pivalolactone); poly(vinylidene fluoride); isothermal spherulitic growth)

INTRODUCTION

Recent studies[1] of the morphology, crystallization and melting behaviour of α-phase poly(pivalolactone), also denoted poly(α,α'-dimethylpropiolactone) or PPVL, in mixtures with poly(vinylidene fluoride) (PVF_2) suggest that this polymer pair is miscible in the molten state over the whole compositional range. Such a result is not surprising as PVF_2 is known to be miscible with a large number of ester-containing polymers, such as poly(methyl methacrylate) (PMMA)[2–10], poly(ethyl methacrylate) (PEMA)[11], poly(ethyl acrylate) (PEA)[4,12], poly(methyl acrylate) (PMA)[13], poly(3-hydroxybutyrate) (PHB)[14,15] and poly(vinyl acetate) (PVAc)[16,17]. On the basis of spectroscopic studies[10] of mixtures of PVF_2 with ester-containing, low molecular weight analogues, the molecular level miscibility in these blends is attributed to hydrogen bonding between the ester carbonyl group of the polyester and the protons of PVF_2. One must emphasize at this point that the PPVL and PMMA repeat units are structural isomers and may be expected on this basis to exhibit interactions with PVF_2 that are similar both in nature and strength. The PPVL/PVF_2 polymer pair is of further interest because it offers a rare opportunity to study the isothermal crystallization of one polymer (i.e. PPVL) from a miscible blend over the whole range of blend compositions and also over a fairly large temperature range (ca. 35–45°C), over which the PVF_2 component remains in the liquid state. This is not the case with other semicrystalline interactive polymer blends where an increase in the content of the non-crystallizable component generally increases the blend glass transition temperature and narrows the crystallization window (see, for example, studies of blends of PVF_2 with PMMA[3], PVAc[16] and poly(vinyl pyrrolidone) (PVP)[18,19], or blends of poly(ethylene oxide) with PMMA[20,21]). Furthermore, the crystallization behaviour of PPVL has been extensively characterized[22–26] and the thermodynamic and

* Presented at 'International Polymer Physics Symposium Honouring Professor John D. Hoffman's 70th Birthday', 15–16 May 1993, Washington, DC, USA

† To whom correspondence should be addressed

0032-3861/94/09/1896–13

crystallographic parameters[27–29] for the PPVL α phase are well documented in the literature. Finally, this polymer mixture constitutes one of the rare examples of a miscible blend from which both components can crystallize upon cooling, thus providing access to a wealth of new morphologies.

The objectives of this work are (i) to investigate the spherulitic growth kinetics of α-phase PPVL from PPVL/PVF_2 blends and (ii) to ascertain the applicability of the Lauritzen–Hoffman kinetic theory of crystal growth[30,31] to the case of crystallization from miscible mixtures. Specifically, we will analyse the temperature dependence of the linear crystal growth rate data for α-phase PPVL from blends of various compositions, from which a simultaneous determination of the composition dependence of the equilibrium melting temperature T_m and the nucleation constant K_g is possible. We will show that such an '*a priori* unconventional' analysis[32] is indeed rigorous and yields values for K_g and T_m for PPVL that are, within the uncertainty limits, identical to those reported earlier[28]. The composition dependence of the surface free energy product $\sigma\sigma_e$ will then be discussed in the context of a recently proposed correlation between the characteristic ratio of a crystallizable polymer chain and the lateral melt/crystal interfacial free energy[33].

THEORETICAL BACKGROUND

We will first briefly review the results of the Lauritzen–Hoffman (LH) kinetic treatment of crystal growth for homopolymers[30,31] and then consider how such a model can be applied to the case of PPVL/PVF_2 blends. According to the LH treatment, the rate of isothermal crystal growth G for a homopolymer is given by

$$G_i = G_i^\circ \exp\left[\frac{-U^*}{R(T_x - T_\infty)}\right] \exp\left[\frac{-K_{g(i)}}{T_x \Delta T f(T_x)}\right] \quad (1)$$

where i = I, II or III qualifies the crystal growth regime, and the undercooling $\Delta T = T_m - T_x$ is the temperature difference between the equilibrium melting temperature T_m and the crystallization temperature T_x. The pre-exponential factor G_i° in equation (1) has a very weak temperature dependence and will be considered constant. The first exponential term accounts for the temperature dependence of the segmental transport across the liquid/solid interface, whereas the second exponential term describes the driving force for crystal growth as expressed under the assumption of a coherent secondary nucleation process. U^* is the activation energy for segmental transport and T_∞ is the temperature below which molecular motions necessary for the transport of segments across the liquid/solid interface become infinitely slow. T_∞ is generally taken as $T_g - 30$ K, although it must be noted that such an expression has only been rigorously tested for isotactic polystyrene[34]. When isothermal crystallization is studied far above the glass transition temperature (PPVL is crystallized at temperatures which are 185 to 245°C above T_g), the exact values of T_∞ and U^* and even the functional form of the transport term do not affect in any significant manner the temperature dependence of the crystal growth rate[30,35] (secondary nucleation control *versus* transport control). According to the LH theory, at low undercooling crystal growth is controlled by a process of coherent secondary nucleation where the nucleation constant $K_{g(i)}$ is given by

$$K_{g(i)} = \frac{2jb_0\sigma\sigma_e T_m}{k\Delta h_f^\circ} \quad (2)$$

where j has a value of 1 for regime II and a value of 2 for regimes I and III, b_0 is the thickness of a monomolecular layer in the direction normal to the growth plane, σ is the lateral crystal/melt interfacial free energy, σ_e is the fold surface free energy, k is Boltzmann's constant, Δh_f° is the enthalpy of fusion of a perfect and infinitely large crystal at its equilibrium melting temperature, and $f(T_x) = 2T_x/(T_m + T_x)$ is a small empirical correction factor accounting for the temperature dependence of the enthalpy of fusion[34]*.

In practice, equation (1) is often written in logarithmic form and a plot of $\ln G + U^*/R(T_x - T_\infty)$ *versus* $1/T_x\Delta T f(T_x)$ can be used to determine the nucleation constant $K_{g(i)}$ from the slope of the straight line in each regime. The ratios of these nucleation constants $K_{g(I)}/K_{g(II)}$ and $K_{g(III)}/K_{g(II)}$ have been predicted[30,36] to be exactly 2. Finally, once the nucleation constants are known (equation (2)), the surface energy product $\sigma\sigma_e$ can be calculated, if the appropriate thermodynamic and crystallographic parameters are available for the crystal form of interest of that polymer. Since the fold surface free energy σ_e can be determined independently of the LH treatment via a purely thermodynamic argument[30], the lateral surface free energy σ can be calculated from the ratio of $\sigma\sigma_e$ and σ_e. The fold surface free energy σ_e is mainly associated with the work of chain folding[30], $q = 2A_0\sigma_e$, and is an indirect measure of the chain stiffness (A_0 is the cross-sectional area of the polymer chain). In contrast with the well accepted physical meaning of the fold surface free energy, the nature of the lateral surface free energy has long eluded researchers in this field. Recently, a treatment of the lateral surface free energy by Hoffman *et al.*[33] has suggested a direct connection between σ, for crystals formed by crystallization from the melt (theta state), and the characteristic ratio of the polymer chain, C_∞. Within this framework, the lateral surface free energy is thought to arise from the entropic penalty incurred by a portion of the polymer chain as it becomes physically adsorbed onto the crystal growth face prior to full crystallographic attachment.

Examination of the literature suggests that the analysis of crystal growth rate data can only yield a meaningful nucleation constant $K_{g(i)}$ if an accurate value for the equilibrium melting temperature is available. One of the two following methods is generally employed to obtain this thermodynamic quantity by an extrapolative procedure. First, the Gibbs–Thomson–Tammann method[29,30], which is based on a thermodynamic argument, utilizes the rigorous correlation between lamellar crystal thickness and crystal stability; the second is the Hoffman–Weeks approach[30,37], which is based on a combination of the previous approach with the correlation between crystal thickness and crystallization temperature, as described by the Lauritzen–Hoffman treatment. In both cases, these approaches must be used with extreme caution with polymers that are not chemically or structurally pure (i.e. copolymers, branched or heterotactic polymers, etc.) or in

*Note that this empirical equation has only been examined for polyethylene and isotactic polystyrene, and that a more rigorous method would require the use of heat capacity data for the liquid and crystal phases in the appropriate crystallization temperature range

polymer systems that exhibit significant lamellar thickening processes either isothermally or during heating. In the case of polymer blends, the likelihood of inhomogeneous distribution of the amorphous component between the lamellae of the crystallizable polymer and inhomogeneous thickening processes poses an additional problem. We will present below a new approach to the analysis of crystal growth rate data which does not require an *a priori* knowledge of the equilibrium melting temperature for the polymer crystal of interest.

Although the LH theory has been utilized in the past to model crystal growth rate data in polymer blends[21,38], there is a need to investigate the validity of such an approach for polymer mixtures. There is also a need for investigations over the widest possible blend composition range so as to maximize the likely effects of blend composition on the thermodynamic and kinetic parameters characterizing the crystallization process (i.e. equilibrium melting temperature, surface energies, activation energy for transport, etc.). For crystallization from miscible blends where specific interactions are present, the equilibrium melting temperature of the crystallizable polymer will be composition dependent and its value will be depressed from that of the pure polymer by an amount which depends on the strength of the specific interactions between the two components [3,39]. For such blends one should also anticipate a blend compositional dependence for both the activation energy for segmental transport across the liquid/solid interface and the glass transition temperature of the solid/liquid interface, if the two components have different T_g values[21,38]. Previous studies[3] on a related system, PVF_2/PMMA, suggest that large equilibrium melting temperature depressions may be observed for PPVL crystals in blends with PVF_2, especially in PVF_2-rich mixtures. The fact that the T_g of the PVF_2 component[40] (ca. -40°C) is only slightly lower than that of PPVL[41] (ca. -3°C), and that both T_g values are far below the temperature range where isothermal crystallization can be studied, led us to assume that the temperature dependence of the α-phase PPVL crystal growth rate will be principally controlled by the secondary nucleation process and will not be affected by potential differences between the diffusional properties of these two polymers. Furthermore, as indicated above, the crystallization of the PPVL component can be observed in a fairly wide temperature range far above T_g but at large enough undercoolings, which are recommended for an unambiguous data analysis, when the equilibrium melting temperatures are not known *a priori* with great accuracy.

EXPERIMENTAL

Poly(pivalolactone) was purchased from Polysciences with a viscosity average molecular weight $M_v = 250\,000$ g mol^{-1}, as measured by intrinsic viscosity in tetrachloroethane/phenol solvent mixtures. The molecular weight distribution[42] for this material was expected to be around 2.0. The PPVL samples were cleaned by consecutive filtration and precipitation of a polymer solution (1 wt% PPVL in benzophenone at 180°C) into distilled deionized water. This process was carried out in the dark and under dry nitrogen flow to minimize polymer and solvent degradation. The precipitate was washed with excess acetone and dried at 120°C for 24 h in a vacuum oven. Poly(vinylidene fluoride), Kynar 710, was kindly supplied by Elf-Atochem North America in pellet form. The number and weight average molecular weights of this polymer were $M_n = 45\,000$ g mol^{-1} and $M_w = 140\,000$ g mol^{-1}, respectively, and the content in regio defects was estimated to be about 5% by ^{19}F n.m.r.[45]. PVF_2 was cleaned by successive filtration and precipitation of a polymer solution (1 wt% PVF_2 in *N*,*N*-dimethylformamide at 80°C) into an ice–water mixture. A dry nitrogen flow was used during dissolution, filtration and precipitation to minimize polymer and solvent degradation. PPVL/PVF_2 blends were prepared by dissolving cleaned PPVL and PVF_2 powders in benzophenone at 180°C. To minimize polymer degradation while ensuring complete dissolution and mixing, the PPVL component was allowed to reside in solution for 30 min and the PVF_2 component for 10 min (under a nitrogen atmosphere and in the absence of light). The homogeneous solution was then precipitated in a water/acetone mixture at 0°C, filtered and washed with excess acetone. The blends were further dried in a vacuum oven at 100°C for 36 h. Thin films for polarized optical microscopy were prepared by melting the dry blend powder between two cover slips at 260°C in a Linkam hot stage for 3 min. The samples were then quenched to the isothermal crystallization temperature T_x, where spherulitic crystal growth was followed in a Zeiss Axioplan polarizing microscope. The temperature scale of the hot stage was calibrated using the melting transition of indium ($T_m = 156.6$°C) at a very slow heating rate. Spherulitic growth rates were measured for α-phase PPVL in the temperature range from 160 to 215°C for various PVF_2 contents in the blend (0, 30, 50, 70, 80 and 90 wt%). In all cases, the isothermal crystallization temperatures were high enough so that the PVF_2 component remained in the liquid state. The spherulitic growth rates were constant until spherulitic impingement for all isothermal crystallization experiments, indicating that rejection of the PVF_2 polymeric diluent into the interspherulitic region did not occur to a significant extent. Although at the lowest crystallization temperature some γ-phase PPVL spherulites were occasionally observed, this study is solely concerned with the investigation of the α-phase crystal growth which is predominant in this temperature range[28].

Differential scanning calorimetry was used to study the melting behaviour of crystals formed under isothermal crystallization of the homopolymer and of blends containing respectively 50 wt% and 10 wt% PPVL. To that end a Perkin–Elmer DSC 2 was used under a dry nitrogen flow at a heating rate of 10°C min^{-1}. The temperature and heat flow rate scales were calibrated in the conventional manner using indium and lead standards. The samples were first melted at 260°C for 3 min, then quenched to suitable isothermal crystallization temperatures. The samples were allowed to crystallize under such conditions so as to achieve 10 wt% crystallinity and heated from that temperature to their melting transition. Peak melting temperatures were then recorded for each crystallization temperature and blend composition so as to carry out the Hoffman–Weeks analysis for each material.

RESULTS

The spherulitic growth rate was calculated as the slope of a radius *versus* crystallization time plot for one to three spherulites, depending on crystallization temperature and nucleation density. Since the crystallization of PPVL is

Table 1 Isothermal growth rate data ($\mu m\ s^{-1}$) for α-phase PPVL in PPVL/PVF_2 blends

PPVL/PVF_2 T_x(°C)	100/0	70/30	50/50	30/70	20/80	10/90
160						0.094
164				0.699		
165					0.221	
166				0.606		0.0701
166.2						0.0699
168				0.521	0.180	
169		3.52				
170		3.03	1.53	0.483	0.147	
170.1						0.0599
171		2.84				
172			1.33	0.393	0.136	0.0574
173						0.0476
174		2.08	1.11	0.303	0.124	0.0438
175				0.248		
176			0.831	0.233	0.0980	0.0400
177		1.49				
178			0.635	0.196	0.0884	0.0368
179						0.0322
180	6.20	1.17	0.491	0.160	0.0746	0.0296
181		0.902				
182			0.419	0.125	0.0587	0.0261
183		0.686			0.0523	
184	3.17		0.312		0.0451	0.0181
185	2.68	0.550	0.269	0.0925	0.0404	0.0176
186	2.40				0.0360	0.0155
187	2.01	0.385	0.171		0.0308	
188				0.0580	0.0269	0.0125
189	1.22				0.0232	
190	0.985	0.265	0.127	0.0405	0.0214	0.00952
191	0.814				0.0191	0.00829
192	0.600	0.174	0.0860	0.0262	0.0154	0.00729
193	0.501				0.0128	
194					0.0104	0.00565
195	0.280	0.0890	0.0400	0.0147	0.00952	
196					0.00803	0.00413
197	0.157	0.0595	0.0247	0.0100	0.00617	0.00321
198					0.00529	
199					0.00422	
200	0.066	0.0300	0.0110	0.0066	0.00419	0.00239
201					0.00296	
202	0.038	0.0153	0.00780	0.0051	0.00281	0.00181
203					0.00211	
204					0.00198	0.00125
205	0.020	0.00850	0.00473	0.0033	0.00157	0.00111
206					0.00130	
207	0.0135	0.00635	0.00320			0.00072
210	0.00745	0.00325	0.00215	0.0010		
211.5	0.00535					
215		0.00155	0.00075			
215.5	0.0022					

characterized by a fairly low nucleation density and the spherulites grow to fairly large dimensions[28], we repeated each crystallization experiment from three to seven times to obtain a reliable average value of the growth rate for each crystallization temperature and blend composition. Although in very few cases the standard deviation around an average growth rate datum reached 8%, it was less than 5% for the great majority of our measurements. The growth rate data for the various blends are listed in *Table 1* and plotted on a logarithmic scale as a function of crystallization temperature T_x in *Figures 1a* to *1f*. These figures show that, at a crystallization temperature of 180°C, the growth rate of PPVL crystals is about 250 times higher in the pure homopolymer than in the 10/90 PPVL/PVF_2 blend, whereas at 205°C the composition dependence of crystal growth rates is less significant (the ratio of the growth rates is only about 20). This observation clearly indicates qualitatively that both the equilibrium melting temperature and the nucleation constants of PPVL are continuously depressed with increasing concentration of PVF_2 in the blends. Careful observation of these data also suggests a clear break in the original growth rate curve of each blend, with the exception of the two most diluted mixtures. A discontinuity in the temperature coefficient of the growth rate curve could in principle be attributed to a change in the crystallographic direction of growth in the crystal phase of the leading lamellae or in the crystallization regime. Earlier studies[28] on pure PPVL indicated that only the latter hypothesis was correct and that a regime II→III transition occurred at 203±2°C. For crystallization of PPVL from the various blends, a study of the crystallization temperature dependence of the PPVL spherulite birefringence by polarized optical microscopy using a retardation plate suggests that there is no obvious change in the average crystal growth direction at the growth transition temperature. Furthermore, examination of the crystallization temperature dependence of the melting transition does not reveal any discontinuity at that growth transition temperature. These observations suggest that such a growth transition is most likely associated with a transition from regime III to regime II crystallization as crystal growth is carried out at increasingly higher temperatures.

GROWTH RATE AND HOFFMAN–WEEKS ANALYSES

The analysis of the temperature dependence of the spherulitic growth rate data in the context of the Lauritzen–Hoffman secondary nucleation hypothesis is generally carried out by plotting $\ln G + U^*/R(T_x - T_\infty)$ *versus* $1/T_x\Delta Tf(T_x)$ (hereafter called the LH plot). Thus, the nucleation constant(s) $K_{g(i)}$ can be obtained if values for T_∞, U^* and T_m are available for the crystallizable polymer. As was discussed above and shown in earlier work[28,35], the estimation of $K_{g(i)}$ from the analysis of growth rate data far from the glass transition temperature is not affected by the choice of the first two quantities (T_∞ and U^*). We will therefore take for U^* the 'universal' value of 1500 cal mol^{-1} (1 cal = 4.2 J) used by Suzuki and Kovacs[34] for isotactic polystyrene and calculate T_∞ for each blend using the classical relationship between T_∞ and T_g. The Fox equation[44,45] for miscible polymer mixtures will be used to estimate the composition dependence of the glass transition temperature of the blend (*Table 2*).

Determination of the equilibrium melting temperature and nucleation constants from the growth rate data

The value of T_m necessary to analyse the growth rate data can in principle be obtained by the Hoffman–Weeks or the Gibbs–Thomson–Tammann method. Whereas the first method cannot be used unambiguously for PPVL because of the time and temperature dependence of the lamellar thickening process[29] (i.e. a Hoffman–Weeks plot exhibits curvature), it can certainly provide a crude estimate of the composition dependence of the equilibrium melting temperature. The second method, which appears *a priori* more reliable, requires measurements of PPVL long spacings above the melting temperature of PVF_2 crystals. Such a study is in progress and will be reported later to confirm some of the assumptions made in the present paper. A third method, presented below, has allowed us to obtain the equilibrium melting temperature of PPVL crystals in blends of various

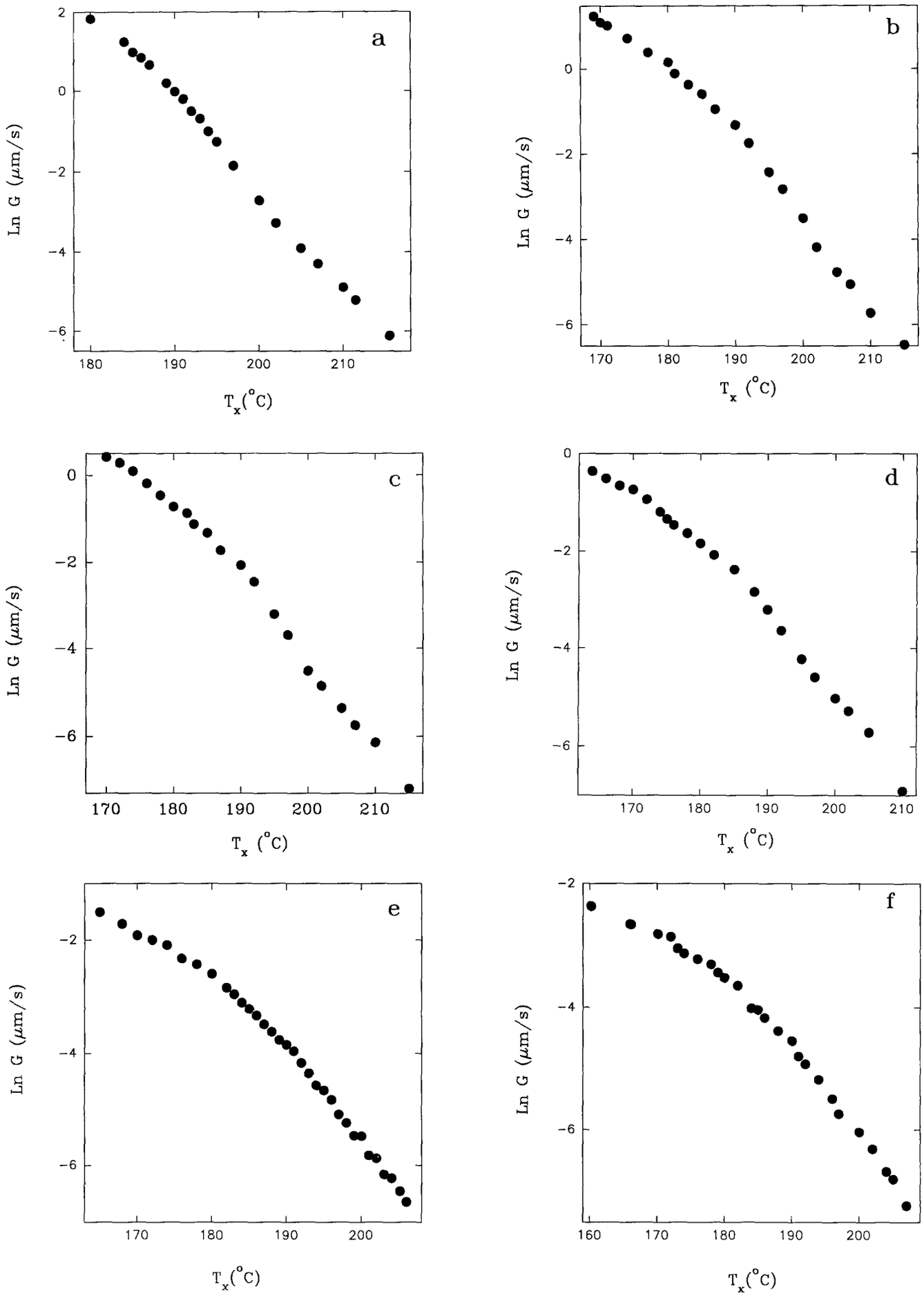

Figure 1 Plots of the natural logarithm of growth rate G *versus* crystallization temperature T_x for (a) 100/0, (b) 70/30, (c) 50/50, (d) 30/70, (e) 20/80 and (f) 10/90 PPVL/PVF$_2$ blends

Table 2 Glass transition temperatures for PPVL/PVF$_2$ blends as a function of blend composition, using the Fox equation and literature values for the glass transition temperatures of PVF$_2$[40] and PPVL[41]

PPVL/PVF$_2$	100/0	70/30	50/50	30/70	20/80	10/90	0/100
T_g(K)	270.2	257.9	250.1	243.1	239.6	236.4	233.2

compositions. This method[32] is based on the single assumption that the growth rate G of a polymer spherulite that has achieved spherical symmetry can be expressed over a certain temperature range (crystallization regime) by the Lauritzen–Hoffman equation. The equilibrium melting temperature T_m is then obtained by trial and error as the temperature T_m for which a plot of $\ln G + U^*/R(T_x - T_\infty)$ *versus* $1/T_x(T_m - T_x)f(T_x)$ is best approximated by a linear function. Specifically, we will use the method of least squares to determine the value of T_m which yields the lowest variance in the linear fit of $\ln G + U^*/R(T_x - T_\infty)$ by the function $\ln G_0 + K_{g(i)}/T_x(T_m - T_x)f(T_x)$. Then $\ln G_0$ and $K_{g(i)}$ are the constants defining the linear fitting function. We will not dwell here on the values obtained for G_0 as this quantity depends markedly on the choice (here *ad hoc*) of U^* and T_∞.

A minor complication arises in the least-squares analysis when multiple crystallization regimes are present, as this method must be applied to individual crystallization regimes and the overall variance minimized. Two approaches were adopted to tackle this problem. First, we used the temperature where the break in the growth rate data was observed experimentally to delineate the different regimes and we applied the least-squares method to each regime to calculate the overall variance for each equilibrium melting temperature. The equilibrium melting temperature was then obtained as that giving the lowest overall variance. Second, we varied arbitrarily the regime transition temperature and repeated the above least-squares process to determine if the choice of transition temperature could affect the estimation of the equilibrium melting temperature T_m. In the following, we will discuss five important results. (i) The least-squares method yields for PPVL an equilibrium melting temperature and nucleation constants which are, within the stated uncertainty, identical to those reported in the literature[28,29] or obtained by the Hoffman–Weeks method. (ii) The ratio of the nucleation constants of α-phase PPVL for each regime is consistent with that found in an earlier study[28] (i.e. about 2.0). One must note that, during the fitting procedure, no constraint is imposed on the ratio of the nucleation constants for each regime. (iii) The equilibrium melting temperature values obtained for the 50/50 and the 10/90 PPVL/PVF$_2$ blends by this new approach are in agreement with those inferred from the Hoffman–Weeks approach. (iv) The blend composition dependence of the equilibrium melting temperature for α-phase PPVL can be successfully analysed by the Nishi–Wang approach to yield an interaction parameter whose magnitude is fully consistent with the results of studies[3] carried out on PVF$_2$/PMMA. (v) We will show that if the regime transition temperature is incorrectly chosen, either the fit of the data by the LH growth rate equation is non-linear or a meaningless equilibrium melting temperature is derived from such a procedure.

PPVL homopolymer. The least-squares method was used with the above PPVL growth rate data using T_m values ranging from 252 to 282°C and assuming the regime II→III transition temperature to be that observed at 203.5±1.5°C. *Figure 2a* shows the dependence of the variance of the fit s^2 on T_m for the pure polymer. A minimum in the variance is observed at $T_m = 269$°C, which is in perfect agreement with our previous estimate of the equilibrium melting temperature for PPVL of 269±2°C by the Gibbs–Thomson–Tammann treatment[29]. The nucleation constants, their ratios and the transition temperatures are listed in *Table 4* and match very well the literature values (*Table 3*). *Figure 3a* displays the LH plot of the isothermal growth rate data for spherulites formed from the pure PPVL melt. It is worth noting that the least-squares procedure produces a very linear plot in each regime without any systematic deviation of the data from the fit.

If the regime transition temperature is chosen in any temperature range above 205°C or below 200°C, unreasonable equilibrium melting temperatures are obtained by minimization of the variance and the LH plots exhibit marked curvature. Various test cases are given in *Table 5* for pure PPVL where the regime transition temperature was chosen in the range from 199 to 207°C. Note that the absolute minimum variance is obtained for a regime II→III transition temperature of 203.5°C and an equilibrium melting temperature of 269°C.

70/30, 50/50 and 30/70 PPVL/PVF$_2$ blends. The least-squares method was first carried out using the observed regime II→III transition temperature (*Table 4*) with input values for the equilibrium melting temperature ranging from 249 to 279°C for the 70/30 blend, from 240 to 270°C for the 50/50 blend and from 235 to 265°C for the 30/70 blend. In each case, the overall variance of the linear fit over the two regimes can be minimized to yield equilibrium melting temperatures for α-phase crystals in the 70/30, 50/50 and 30/70 blends given in *Table 4* (see *Figures 2b* to *2d* for the plots of variance *versus* equilibrium melting temperature). Nucleation constants are also given in *Table 4* for each regime of the various blend compositions. The LH plots for these blends shown in *Figures 3b* to *3d* do not exhibit any curvature in either regime.

As in the case of pure PPVL, varying the value of the regime transition temperature or analysing the data without a regime transition did not result in a physically meaningful minimization of the variance. If we adopted a regime transition temperature that differed greatly from the observed value, very high equilibrium melting temperatures were obtained by minimization of the variance and the LH plots were not linear but curved. On the other hand, if we chose regime transition temperatures not too distant from the observed value, the resulting equilibrium melting temperature was lower but the LH plot was still curved. Only when we adopted the experimentally observed regime transition temperature could we minimize the variance and obtain linear LH plots. In *Table 5* are listed the equilibrium melting temperatures obtained by minimization of the variance for various blend compositions and different choices of the regime transition temperature.

20/80 and 10/90 PPVL/PVF$_2$ blends. The growth rate curve for each of these two blends does not exhibit a clear regime transition. If we analyse the data by assuming a single regime over the whole temperature

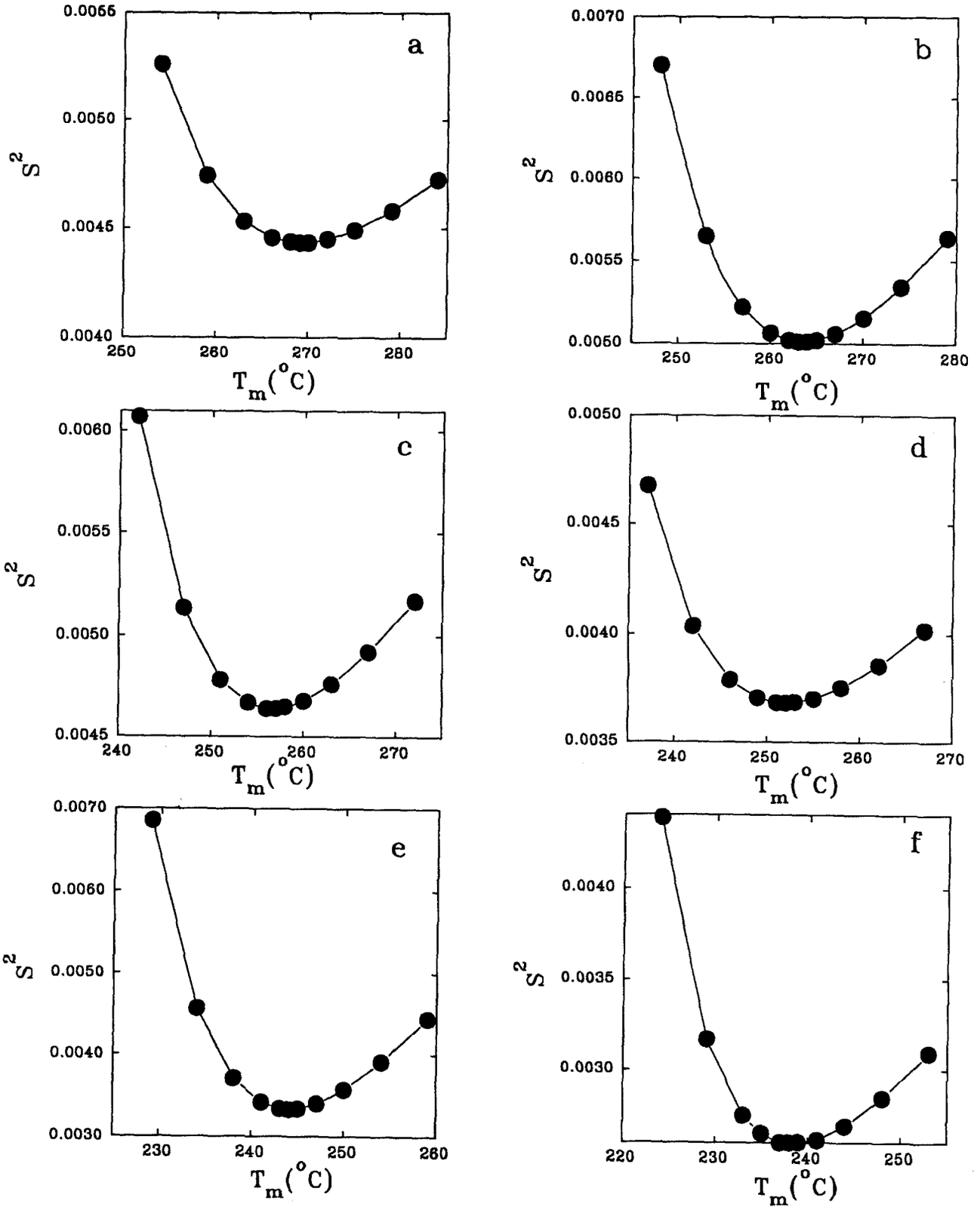

Figure 2 Plots of the variance s^2 of the fit of $\ln G + U^*/R(T_x - T_\infty)$ by $1/T_x\Delta Tf(T_x)$ as a function of the equilibrium melting temperature T_m for (a) 100/0, (b) 70/30, (c) 50/50, (d) 30/70, (e) 20/80 and (f) 10/90 PPVL/PVF_2 blends

range, the variance of the fit can be minimized to yield equilibrium melting temperatures of 281°C for the 20/80 blend and 275°C for the 10/90 blend. Such values for T_m are higher than that of pure PPVL and are clearly unacceptable on thermodynamic grounds. Furthermore, the LH plots derived from such equilibrium melting temperatures exhibit a marked curvature. We then carried out the least-squares analysis by assuming various regime transition temperatures in the range from 160 to 205°C. For these blends, it is possible to minimize the variance and obtain linear LH fits to the data for various transition temperatures. In view of the ambiguity of such results, we decided to minimize the variance of the fit with respect to both the equilibrium melting temperature

Table 3 Thermodynamic and structural constants for PPVL and PVF_2

	PPVL			PVF_2	
T_m (°C)	269±2	(ref. 29)			
Δh_f^0 (J cm^{-3})	183.7	(ref. 23)			
Δh_{fu}° (kcal mol^{-1})	3.98	(ref. 23)			
b_0 (nm)	0.574	(ref. 28)			
$K_{g(II)}$ (K^2)	4.32×10^5	(ref. 28)			
$K_{g(III)}$ (K^2)	8.59×10^5	(ref. 28)			
ρ_a (g cm^{-3})	1.18	(ref. 23)	ρ_a (g cm^{-3})	1.60	(ref. 46)
V_{cu} (cm^3 mol^{-1})	84.75	(ref. 23)	V_{au} (cm^3 mol^{-1})	40.0	(ref. 46)

Table 4 PPVL equilibrium melting temperatures, regime transition temperatures, nucleation constants, nucleation constant ratios, interfacial free energy products and lateral melt/crystal interfacial free energies in blends with PVF_2

PPVL/PVF_2	100/0	70/30	50/50	30/70	20/80	10/90
T_m (°C) (Growth rate)	269.0±3.0	263.5±2.5	257.0±2.0	252.0±2.5	244.0±1.5	238.0±2.0
T_m (°C) (Hoffman–Weeks)	265±4		254±4			238±4
$T_{II\to III}$ (°C)	203.5±1.5	201.0±1.0	198.5±1.5	193.5±1.5	200.0±1.0	193.0±1.0
$10^{-5}K_{g(II)}$ (K^2)	4.30±0.5	3.0±0.3	2.2±0.3	2.1±0.2	1.77±0.15	1.1±0.1
$10^{-5}K_{g(III)}$ (K^2)	8.7±0.7	5.9±0.4	4.5±0.5	4.0±0.4	2.82±0.15	1.8±0.1
$K_{g(III)}/K_{g(II)}$	2.02±0.06	1.95±0.04	2.04±0.04	1.91±0.05	1.60±0.05	1.64±0.05
$\sigma\sigma_e$ (erg^2 cm^{-4})	1760±160	1220±100	990±70	790±60	680±110	430±70
σ (erg cm^{-2})	28.8±3.0	20.0±2.0	16.3±1.0	13.0±1.0	11.1±2.0	7.1±1.0
α_{FF}	1.00	1.20±0.05	1.33±0.05	1.49±0.05	1.61±0.09	2.01±0.08

and the regime transition temperature. When the regime transition temperatures were taken as 200°C and 195°C for the 20/80 and 10/90 PPVL/PVF_2 blends, respectively, the variance of the fit was the lowest (*Figures 2e* and *2f*). The PPVL equilibrium melting temperatures for these two blends were then determined to be 244°C and 238°C, respectively. The corresponding values for the nucleation constants are listed in *Table 4*. The LH plots for these two blends shown in *Figure 3e* and *3f* do not show any curvature. The equilibrium melting temperatures obtained by minimization of the variance for various choices of regime transition temperature are given in *Table 5*.

Equilibrium melting temperatures from the Hoffman–Weeks analysis

The plots of observed melting temperature *versus* crystallization temperature are shown in *Figure 4* for pure PPVL and the 50/50 and 10/90 PPVL/PVF_2 blends. As discussed earlier, such plots were expected to show some curvature because of the temperature and time dependence of the lamellar thickening process[29]. In analogy with studies on polyethylene, where thickening becomes very important at the highest crystallization temperatures[47], we elected to carry out the extrapolation to the $T_m' = T_x$ equilibrium line using principally the low crystallization temperature data. Such an approach, although qualitative, may be justified if we consider that isothermal thickening will be more subdued at the lowest crystallization temperatures. Extrapolation to the equilibrium line then provides an estimate for the equilibrium melting temperature of PPVL in the various blends (see *Table 4*).

Equilibrium melting temperature depression

Upon blending a crystallizable polymer (PPVL) with a high molecular weight polymeric diluent (PVF_2), a depression in the equilibrium melting temperature of the crystallizable polymer will be observed in the absence of combinatorial entropic effects if the chemical potential of this polymer in the molecularly mixed liquid state is lowered beyond that of the pure state as a result of specific interactions with the diluent. An expression relating the equilibrium melting temperature depression to the blend composition and the strength of interactions has been obtained by Nishi and Wang[3] for high molecular weight polymers through a simple combination of thermodynamic arguments for mixing (Flory–Huggins theory) and for crystal melting

$$\frac{1}{T_m^\circ} - \frac{1}{T_m} = \frac{RV_{cu}}{\Delta h_{fu}^\circ V_{au}}\chi v_a^2 \tag{3}$$

where T_m° is the equilibrium melting temperature of pure PPVL, T_m is the equilibrium melting temperature for PPVL in the blend containing a volume fraction v_a of PVF_2, Δh_{fu}° is the heat of fusion of PPVL per mole of repeat unit at the equilibrium melting temperature, V_{cu} and V_{au} are, respectively, the molar volumes per repeat unit of crystallizable and amorphous polymer, R is the universal gas constant and χ is the Flory–Huggins interaction parameter. Using the values for molar volumes and heat of fusion available in the literature (*Table 3*) and the equilibrium melting temperature for PPVL in each blend (*Table 4*), one can plot the left-hand

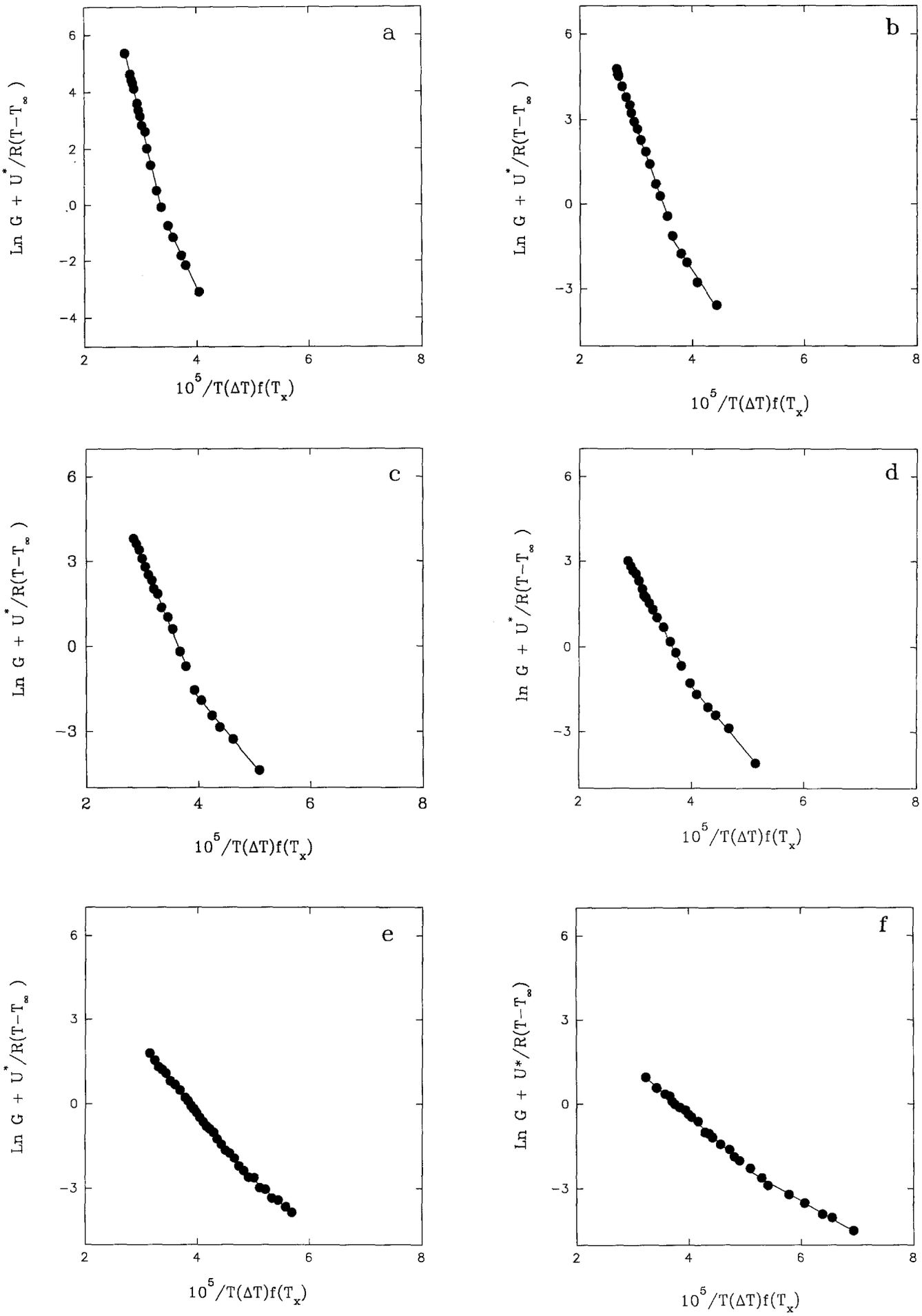

Figure 3 Plots of $\ln G + U^*/R(T_x - T_\infty)$ *versus* $1/T_x\Delta T f(T_x)$ for (a) 100/0, (b) 70/30, (c) 50/50, (d) 30/70, (e) 20/80 and (f) 10/90 PPVL/PVF$_2$ blends

Table 5 Variation in the equilibrium melting temperature obtained by minimization of the variance s^2 with the regime transition temperature for the different PPVL/PVF$_2$ blends[a]

100/0			70/30			50/50			30/70			20/80			10/90		
$T_{II\infty III}$ (°C)	T_m (°C)	Curvature	$T_{II\rightarrow III}$ (°C)	T_m (°C)	Curvature	$T_{II\rightarrow III}$ (°C)	T_m (°C)	Curvature	$T_{II\rightarrow III}$ (°C)	T_m (°C)	Curvature	$T_{II\rightarrow III}$ (°C)	T_m (°C)	Curvature	$T_{II\rightarrow III}$ (°C)	T_m (°C)	Curvature
199.5	>400	Yes	193.5	>400	Yes	191.0	>350	Yes	186.5	>350	Yes	190.5	>400	No	190.5	252	No
201.0	~260	Yes	198.5	>400	Yes	196.0	>350	Yes	191.0	>400	Yes	196.0	253.0	No	191.5	245	No
203.5*	269.0	No	201.0*	263.5	No	198.5*	257.0	No	193.5*	252	No	197.0	251.0	No	195.0*	238	No
206.0	>300	Yes	203.5	251.0	Yes	201.0	~245	Yes	196.0	245	Yes	198.0	245.0	No	196.5	240	No
			206.0	260.0	Yes	203.5	>350	Yes	201.0	>390	Yes	199.0	245.0	No	198.5	245	No
												201.0*	244.0	No	201.0	252	No
												202.0	250.0	No			
												203.0	250.0	No			

[a] The regime II→III transition temperature yielding the lowest variance is marked by *. Note that both the variance and the equilibrium melting temperature obtained during the minimization of the variance increase as the regime transition temperature departs more and more from T^*. The yes/no entries in the curvature columns refer to whether or not the LH plots were curved instead of being straight lines

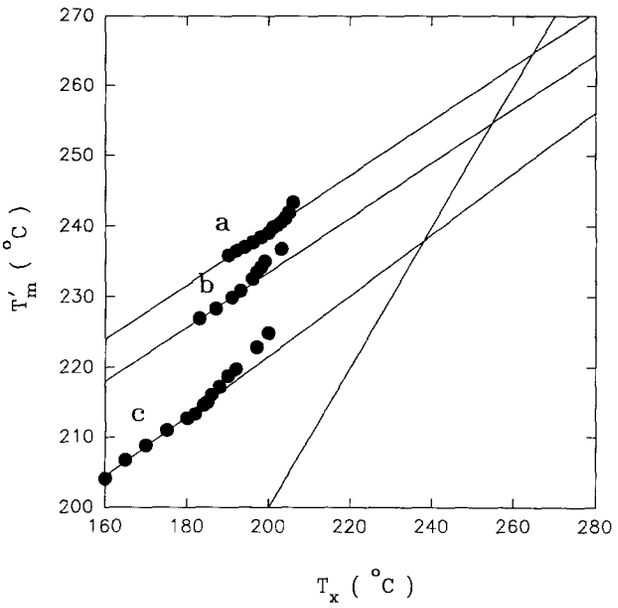

Figure 4 Hoffman–Weeks plots of the observed melting temperature T'_m *versus* crystallization temperature T_x for (a) 100/0, (b) 50/50 and (c) 10/90 PPVL/PVF$_2$ blends

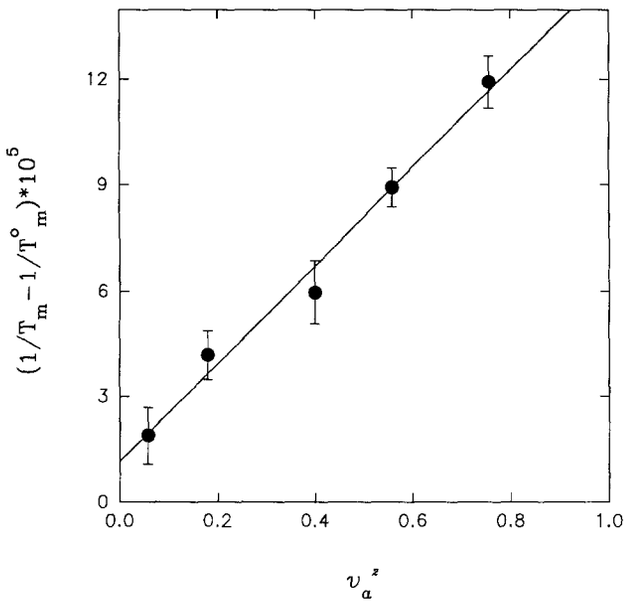

Figure 5 Plot of $1/T_m - 1/T^\circ_m$ *versus* v_a^2 following the approach of Nishi and Wang[3]

side of equation (3) *versus* the square of the PVF$_2$ volume fraction in the blend. Such a plot, shown in *Figure 5*, is linear within the uncertainty in the equilibrium melting temperature. From its slope, the Flory–Huggins interaction parameter $\chi = -0.13 \pm 0.05$.

DISCUSSION

Examination of *Table 4* suggests a continuous decrease in the equilibrium melting temperature of PPVL in blends containing larger amounts of the PVF$_2$ component. The equilibrium melting temperatures obtained by the least-squares analysis and by the less rigorous Hoffman–Weeks method are judged to be self-consistent within the uncertainty of the measurements and the chosen approaches. More importantly, the use of independent least-squares analyses with the various PPVL blends yields smooth and continuous variations in the equilibrium melting temperature and nucleation constants with blend composition. Such an equilibrium melting temperature depression has been successfully analysed using the Nishi–Wang approach to provide a value for the Flory–Huggins interaction parameter $\chi = -0.13$ at a temperature around 250°C. As poly(pivalolactone) and poly(methyl methacrylate) are chemically isomorphous, their respective interactions with poly(vinylidene fluoride) should be qualitatively similar. Studies by Nishi and Wang[3] suggest that the interaction parameter for the PVF$_2$/PMMA blend is equal to -0.3 at 160°C. Since both polymer pairs are expected to interact through hydrogen bond formation, it is likely that they should both exhibit a lower critical solution temperature (*LCST*) behaviour[13]. For polymer mixtures exhibiting specific interactions, one expects the Flory–Huggins interaction parameter to increase with increasing temperature as the favourable enthalpy of mixing would become less negative at higher temperatures because of increased molecular motion[45]. Assuming that the hydrogen bond strength between the PVF$_2$ hydrogen atoms and the ester carbonyls is of the same magnitude in PMMA/PVF$_2$ and in PPVL/PVF$_2$, it is then reasonable to observe a decrease in the χ parameter as we compare these two blends, since the χ of the former mixture is measured at a lower temperature than that of the latter.

Using equation (2) for the nucleation constant $K_{g(i)}$,

the equilibrium melting temperatures in *Table 4* and the various material constants given in *Table 3*, one can then calculate the surface free energy product $\sigma\sigma_e$ as a function of blend composition (*Table 4*). Note that we have assumed that the plane of crystal growth for PPVL in the blends was the same ($1\bar{2}0$) plane as in the case of pure PPVL[28]. The surface free energy product is observed to decrease by a factor of 4.1 between the pure homopolymer and the 10/90 PPVL/PVF_2 blend. A logical question is then concerned with the physical origin for the large decrease in $\sigma\sigma_e$. Considering first the fold surface free energy σ_e, one is tempted to assume it to be independent of composition as this quantity is mainly intramolecular in origin[30]. One must, however, recognize that fold surfaces may under specific circumstances be swollen by the second component[48–50] and exhibit a variable fold surface free energy[51]. Whereas monomeric diluents may mix with chain segments in the fold interface so as to maximize the entropy of mixing, polymeric diluents may not experience the same driving force to penetrate the fold interface as the entropy gain would be minimal. Computer simulations by Kumar and Yoon[52,53] suggest that the fold interfacial region in blends of crystallizable and amorphous high molecular weight polymers should be devoid of the amorphous polymeric diluent unless the specific interactions in the mixture are very favourable. In the case of PVF_2/PMMA blends, dielectric[54,55] and scattering[54,56] experiments have shown that the PMMA component is rejected from the interface between the melt and the crystal fold plane. Similar observations were also made on PEO/PMMA blends[57,58]. Since the PPVL/PVF_2 blend exhibits a lower Flory–Huggins interaction parameter than the PVF_2/PMMA blend, one should also expect the PVF_2 component to be rejected from the melt/crystal interface of the PPVL crystals. If one now considers the effect of chain folding on the change in the total enthalpy of mixing in the blend, one may reach a slightly different conclusion. Upon exclusion of the amorphous component from the fold interface, the number of favourable specific interactions between PPVL segments in the fold and PVF_2 segments in the interface would diminish. The folding process which would result in a lesser amount of specific interactions between unlike repeat units would thus be more energy costly than in the case of pure PPVL. Such a process would then lead to a slight increase in the fold surface free energy as the PVF_2 concentration is increased in the blend. In view of the rather weak hydrogen bonding between unlike repeat units and the rather high energy associated with the chain-folding process[29] ($q = 7.5\,\text{kcal mol}^{-1}$ repeat units), we speculate that the fold surface free energy will not be affected markedly by blend composition. Under such an assumption*, the composition dependence of the surface free energy product must be attributed to the lateral crystal interfacial free energy σ.

We will now turn to the recently suggested correlation[33] between σ and the chain characteristic ratio C_∞ for crystallization from the melt. Such a model is based on the assumption that polymer chains in a pure melt adopt the unperturbed dimensions characteristic of the theta state and that the rate-determining step in the secondary nucleation process is the physical adsorption of an amorphous chain onto the crystal growth front. In this adsorption process only a very small number of segments are expected to come into crystallographic registration with the existing crystal surface, while most of the adjoining segments exhibit (restricted) conformational freedom. This localization or enhanced structure of the adsorbed chain would correspond to an entropy penalty (activation barrier) incurred during nucleation. Such structure enhancement of entropic repulsion has been observed by Dill *et al.*[59] in recent computer simulations. The correlation between σ and C_∞ is then obtained by equating the free energy of activation of entropic nature with the classical $2b_0 l\sigma$ term in the LH theory[30] for the deposition of the first stem on the crystal growth front. The characteristic ratio enters this equation as a scaling parameter between the entropic barrier and the entropy of crystallization for crystallization from the theta state. Under such conditions the lateral surface free energy σ is inversely proportional to C_∞.

When crystallization occurs from a mixture that departs from the theta state, the mean squared end to end distance of the crystallizing chain differs from that of the unperturbed chain by a factor α_{FF} which accounts for the swelling of that polymer chain by the diluent[60]. The expansion ratio α_{FF} is related to the mean squared end to end distance for PPVL chains in the PVF_2 diluent $\langle r^2 \rangle$ and the mean squared end to end distance for PPVL chains in the theta state $\langle r^2 \rangle_0$ by

$$\alpha_{FF}^2 = \frac{\langle r^2 \rangle}{\langle r^2 \rangle_0}$$

Using the correlation between the lateral surface free energy for pure PPVL and the PPVL characteristic ratio, one may then directly obtain a relationship between the lateral surface free energies for PPVL crystals grown from the pure and mixed melts, i.e. σ_0 and σ_ϕ, respectively

$$\alpha_{FF} = \left(\frac{\sigma_{\phi=0}}{\sigma_\phi} \right)^{1/2}$$

Values of the expansion ratio for the PPVL chain were calculated with the above equation and are listed in *Table 4* for the various blend compositions. In view of the rather modest molecular weight of the PPVL chains and the rather weak interactions between unlike repeat units, it is clear that the calculated expansion ratios are much too large to be credible[61]. In the above approach, we only considered the effect of the blend composition on the size of the chain in the liquid state prior to adsorption onto the crystal growth front. In view of the failure of this approach, one must recognize that the structure of the melt/crystal lateral interface may also depend on the blend composition. Since considering only the effect of mixing in the amorphous phase (prior to physical adsorption) on the lateral surface free energy is not sufficient to account for the composition dependence of the lateral surface free energy, it is important to investigate the role of mixing thermodynamics in the physical adsorption process. If we denote by i the initial state of a polymer chain prior to adsorption and by ii the adsorbed or transition state, the free energy change between states i and ii is given by

$$\Delta G_{i \to ii} = \Delta G_{i \to ii}^{\text{demix}} + \Delta G_{i \to ii}^{\text{conf}} \quad (4)$$

where the first term on the right-hand side of equation (4) is the free energy associated with the demixing of PPVL chains as they diffuse from the mixed liquid

* Note that if σ_e increased with PVF_2 concentration, the variation in lateral melt/crystal surface free energy would be even greater

containing a PPVL volume fraction of ϕ_{PPVL}^{bulk} into the lateral crystal/liquid interface containing a volume fraction ϕ_{PPVL}^{intfc}, and the second term on the right-hand side of equation (4) is the free energy associated with the localization of chain segments onto the crystal surface. The first free energy term may be modelled using the Flory–Huggins equation for demixing[60], whereas the second can be rewritten in the following form

$$\Delta G_{i\to ii}^{conf} = -TS_{ii}^{conf} + TS_{i}^{conf} \quad (5)$$

Here, we have assumed that there is no enthalpic contribution to this free energy term; that is, we neglect the enthalpy change associated with the crystallization of the few segments adsorbed in crystallographic registration. The argument is analogous to the consideration of a low value for the apportionment of the free energy of crystallization during deposition of the first stem (low ψ value in the context of the LH theory)[31]. Using equations (4) and (5), and noting that in the context of the LH theory the free energy term on the left-hand side of equation (4) is equal to $2b_0l_u\sigma$, one may then write

$$2b_0l_u\sigma = \Delta G_{i\to ii}^{demix} - TS_{ii}^{conf} + TS_{i}^{conf} \quad (6)$$

where l_u is the projected length of the repeat unit along the c axis. Using equation (6), one can now discuss qualitatively the effect of blend composition on the lateral surface free energy σ. Using the free energy of mixing expression given by the Flory–Huggins theory for polymer blends[45], one can show, to a first approximation, that the free energy of demixing incurred by a PPVL chain as it becomes adsorbed in the lateral interfacial region increases with the difference in the PPVL volume fraction between the interface and the bulk liquid ($\phi_{PPVL}^{intfc} - \phi_{PPVL}^{bulk}$). The magnitude of the free energy of demixing would be of the order of 10 kJ mol^{-1} for PPVL repeat units if we assume $\phi_{PPVL}^{intfc} = 0.9$ and $\phi_{PPVL}^{bulk} = 0.1$. This would correspond to the hypothetical case of a 10/90 PPVL/PVF_2 blend in which the lateral crystal/melt interface is almost a pure (90%) PPVL phase. Such a situation would not favour the secondary nucleation process as it would be associated with too large a value for σ (see equation (6)). This free energy of demixing term can be compared on a mole of repeat units basis to the surface free energy term $2b_0l_u\sigma$, which decreases from 6.04 kJ mol^{-1} for pure PPVL to 1.5 kJ mol^{-1} for the 10/90 blend. One possible way to account for the observed decrease in σ with increase in PVF_2 content in the blend is to propose that the degree of anisotropy (or the flattening) of a PPVL chain adsorbed at the melt/crystal interface decreases as the PVF_2 concentration increases. According to this scenario, a PPVL chain would experience less of an entropic barrier as it becomes adsorbed, or, in other words, its conformational entropy in the interface would be larger in the case of a blend than in pure PPVL. The larger radius of gyration of the adsorbed PPVL chain normal to the growth front would allow more frequent excursions of PPVL chain segments in the bulk liquid where the PVF_2 concentration is the highest. Such a situation would then lead to a much lower free energy of demixing for the loosely adsorbed PPVL chain than for a PPVL chain collapsed on the lateral crystal surface. The increase in PVF_2 concentration should also slightly decrease the conformational entropy of the PPVL chain in the bulk liquid state prior to adsorption as the hydrogen-bonding interactions between unlike repeat units would slightly swell the PPVL coils. The proposal of an increase in melt/crystal lateral interface thickness with PVF_2 concentration in the blend would allow for a minimization of the free energy of demixing during adsorption and a decrease in the entropy difference between the bulk liquid and the interface. Such a process may account for the variation in lateral surface energy with blend composition. In this model we rationalize the variation in σ with blend composition on the basis of maximization of the entropy in the interface and minimization of the free energy of demixing. Such a model relies heavily on the existence of specific interactions between the two components and needs to be further tested by studying the effect of the strength of the specific interactions on the magnitude of the decrease in the lateral surface free energy. Such experiments are in progress for mixtures of poly(pivalolactone) and random copolymers of vinylidene fluoride and tetrafluoroethylene and mixtures of fractions of isotactic and atactic polystyrenes.

NOTE OF CAUTION

Although further details on the application and limitations of the above least-squares method in the analysis of growth rate data will be published separately[32], it is extremely important to note that this method seems to be only applicable when four requirements are satisfied: (i) growth rates must be measured in a temperature range far from the glass transition temperature to ensure that the influence of segmental diffusion across the liquid/solid interface on the growth rate temperature coefficient is negligible; (ii) the growth rate data must be obtained in a sufficiently wide temperature range (here between 35 and 45°C); (iii) the number of data points for each fit must be sufficiently large (here between 19 and 33 data points); and (iv) the growth rate measurements should exhibit the least possible amount of scatter. Although these requirements may seem to preclude the general use of this method as a 'short-cut' approach to determine equilibrium melting temperatures, it can certainly prove valuable for cases where T_m values are difficult to obtain. Furthermore, the success of this method brings further credibility to the $\ln G \propto 1/T_x(T_m - T_x)$ relationship between undercooling and spherulitic growth rate far from the glass transition temperature.

CONCLUSION

Analysis of the temperature dependence of the spherulitic growth rates of α-phase poly(pivalolactone) in blends with poly(vinylidene fluoride) allows us to assess the variations in the equilibrium melting temperature, the nucleation constants and the surface free energy product of PPVL crystals with PVF_2 concentration in the blends. The estimated composition dependence of the PPVL α-phase crystal equilibrium melting temperature can then be analysed using the Nishi–Wang approach to yield the Flory–Huggins interaction parameter ($\chi = -0.13 \pm 0.05$), whose magnitude is consistent with the values obtained in studies of PVF_2/PMMA blends. Independent evaluation of the depression in the PPVL equilibrium melting temperature for various blend compositions using the Hoffman–Weeks approach yields results that are consistent with our kinetic approach. These two observations demonstrate the soundness of this new approach to the determination of equilibrium melting temperatures. These results also clearly indicate that the Lauritzen–Hoffman

treatment of crystal growth is applicable to the blends studied here and that it provides results that are consistent with the thermodynamic arguments derived from the Flory–Huggins theory. Independent determinations of the composition dependence of the equilibrium melting temperature of PPVL crystals and of the Flory–Huggins interaction parameter in PPVL/PVF$_2$ blends, via small-angle X-ray scattering, are in progress and will enable us to test the validity of the surface nucleation arguments presented here. An attempt was also made to relate qualitatively the composition dependence of the PPVL crystal lateral surface free energy to variations in the chain conformational properties both in the melt away from the growth front and in the lateral melt/crystal interface region. A model based on the increase in PPVL melt/crystal lateral interface thickness with PVF$_2$ concentration may account for the decrease in lateral interfacial free energy with PVF$_2$ concentration through a minimization of the free energy of demixing and an increase in the conformational entropy of the chain adsorbed at the melt/crystal interface.

ACKNOWLEDGEMENTS

Acknowledgement is made to the donors of the Petroleum Research Fund, administered by the American Chemical Society, for full support of this research through grant ACS-PRF 23533-AC7.

REFERENCES

1 Bakhshandehfar, R. and Marand, H. *Bull. Am. Phys. Soc.* 1991, **36**, 794
2 Noland, J. S., Hsu, N. N.-C., Saxon, R. and Schmitt, J. M. *Adv. Chem. Ser.* 1971, **99**, 15
3 Nishi, I. and Wang, T. T. *Macromolecules* 1975, **8**, 909
4 Wahrmund, D. C., Bernstein, R. E., Barlow, J. W. and Paul, D. R. *Polym. Eng. Sci.* 1978, **18**, 677
5 Paul, D. R., Barlow, J. W., Bernstein, R. E. and Wahrmund, D. C. *Polym. Eng. Sci.* 1978, **18**, 1225
6 Wendorff, J. H. *J. Polym. Sci., Polym. Lett. Edn* 1980, **18**, 439
7 Hadziioannou, G. and Stein, R. S. *Macromolecules* 1984, **17**, 567
8 Coleman, M. M., Zarian, J., Varnell, D. F. and Painter, P. C. *J. Polym. Sci., Polym. Lett. Edn* 1977, **15**, 745
9 Roerdink, E. and Challa, G. *Polymer* 1980, **21**, 509
10 Leonard, C., Halary, J. L. and Monnerie, L. *Polymer* 1985, **26**, 1507
11 Kwei, T. K., Patterson, G. D. and Wang, T. T. *Macromolecules* 1976, **9**, 780
12 Briber, R. M. and Khoury, F. *Polymer* 1987, **28**, 38
13 Bernstein, R. E., Cruz, C. A., Paul, D. R. and Barlow, J. W. *Macromolecules* 1977, **10**, 681
14 Marand, H. and Collins, M. B. *ACS Polym. Prepr.* 1990, **31**(1), 552
15 Edie, S. L., Prasad, A., Collins, M. B. and Marand, H. *ACS Polym. Prepr.* 1991, **32**(2), 786
16 Bernstein, R. E., Paul, D. R. and Barlow, J. W. *Polym. Eng. Sci.* 1978, **18**, 683
17 Belke, R. E. and Cabasso, I. *Polymer* 1988, **29**, 1831
18 Galin, M. *Makromol. Chem., Rapid Commun.* 1984, **5**, 119
19 Alfonso, G. C., Turturro, M., Pizzoli, M. A., Scandola, M. and Ceccorulli, G. *J. Polym. Sci., Polym. Phys. Edn* 1989, **27**, 1195
20 Martuscelli, E., Pracella, E. and Yue, W. P. *Polymer* 1984, **25**, 1097
21 Alfonso, G. C. and Russell, T. P. *Macromolecules* 1986, **19**, 1143
22 Ferro, D. R., Brückner, S., Meille, S. V. and Ragazzi, M. *Macromolecules* 1990, **23**, 1676
23 Borri, C., Brückner, S., Crescenzi, V., Della Fortuna, G., Mariano, A. and Scarazzato, P. *Eur. Polym. J.* 1971, **7**, 1515
24 Prud'homme, R. E. and Marchessault, R. H. *Makromol. Chem.* 1974, **175**, 2705
25 Noah, J. and Prud'homme, R. E. *Eur. Polym. J.* 1981, **17**, 353
26 Meille, S. V., Konishi, T. and Geil, P. H. *Polymer* 1984, **25**, 773
27 Perego, G., Melis, A. and Cesari, M. *Makromol. Chem.* 1972, **157**, 269
28 Roitman, D. B., Marand, H., Miller, R. L. and Hoffman, J. D. *J. Phys. Chem.* 1989, **93**, 6919
29 Marand, H. and Hoffman, J. D. *Macromolecules* 1990, **23**, 3682
30 Hoffman, J. D., Davis, G. T. and Lauritzen Jr, J. I. in 'Treatise on Solid State Chemistry' (Ed. N. B. Hannay), Vol. 3, Plenum Press, New York, 1976, Ch. 7
31 Hoffman, J. D. and Miller, R. L. *Macromolecules* 1988, **21**, 3038
32 Marand, H., Reinhard, D. M., Huang, J. and Celarier, E. in preparation
33 Hoffman, J. D., Miller, R. L., Marand, H. and Roitman, D. B. *Macromolecules* 1992, **25**, 2221
34 Suzuki, T. and Kovacs, A. J. *Polym. J.* 1970, **1**, 82
35 Miller, R. L. in 'Flow Induced Crystallization' (Ed. S. E. Keinath), Gordon and Breach, Reading, 1979
36 Hoffman, J. D. *Polymer* 1983, **24**, 3
37 Hoffman, J. D. and Weeks, J. J. *J. Res. Natl Bur. Stand.* 1962, **66**, 13
38 Saito, H., Okada, T., Hamane, T. and Inoue, T. *Macromolecules* 1991, **24**, 4446
39 Rostami, S. *Polymer* 1990, **31**, 899
40 Hsu, C. C. and Geil, P. H. *J. Appl. Phys.* 1984, **56**, 2404
41 Pratt, C. F. and Geil, P. H. *J. Macromol. Sci., Phys.* 1982, **21**, 617
42 Beckerbauer, R. Personal communication, 1992
43 Pennwalt Corporation, King of Prussia, PA, manufacturer's data
44 Fox, T. G. *Bull. Am. Phys. Soc* 1956, **1**, 123
45 Paul, D. R. and Newman, S. (Eds) 'Polymer Blends', Vol. 1, Academic Press, New York, 1978, Ch. 2, p. 20
46 Welch, G. J. and Miller, R. L. *J. Polym. Sci., Polym. Phys. Edn* 1976, **14**, 1683
47 Weeks, J. J. *Res. Natl Bur. Stand., Sect. A* 1963, **67**, 441
48 Udagawa, Y. and Keller, A. *J. Polym. Sci. (A-2)* 1971, **9**, 437
49 Ergöz, E. and Mandelkern, L. *J. Polym. Sci., Polym. Lett. Edn* 1972, **10**, 631
50 Harrison, I. R., Weaver, T. J. and Runt, J. *Polymer* 1985, **26**, 244
51 Nakajima, A., Hamada, F., Hayashi, S. and Sumida, T. *Kolloid Z. Z. Polym.* 1968, **222**, 10
52 Kumar, S. K. and Yoon, D. Y. *Macromolecules* 1989, **22**, 4098
53 Kumar, S. K. and Yoon, D. Y. *Macromolecules* 1991, **24**, 5414
54 Hahn, B., Wendorff, J. and Yoon, D. Y. *Macromolecules* 1985, **18**, 718
55 Hahn, B. R., Herrmann-Schönherr, O. and Wendorff, J. H. *Polymer* 1987, **28**, 201
56 Yoon, D. Y., Ando, Y., Rojstaczer, S., Kumar, S. K. and Alfonso, G. C. *Makromol. Chem., Macromol. Symp.* 1991, **50**, 183
57 Russell, T. P., Ito, H. and Wignall, G. D. *Macromolecules* 1988, **21**, 1703
58 Runt, J. P., Barron, C. A., Zhang, X.-Y. and Kumar, S. K. *Macromolecules* 1991, **24**, 3466
59 Chan, H. S., Wattenbarger, M. R., Bloomfield, V. A. and Dill, K. A. *J. Chem. Phys.* 1991, **94**, 8542
60 Flory, P. J. 'Principles of Polymer Chemistry', Cornell University Press, Ithaca, NY, 1953, Ch. XII, p. 495
61 Shultz, A. R. and Stockmeier, W. H. *Macromolecules* 1969, **2**, 178